Railway Sciences

625

Improving the activity of waste concrete recycled powder by a mechanical-microwave combing method

Henan Shi, Huajian Li, Liangshun Li, Haoliang Dong, Zhen Wang and Wenxiao Ji

China Academy of Railway Sciences Corporation Limited, Railway Engineering Research Institute, Beijing, China and State Key Laboratory of High Speed Railway Track System, Beijing, China

Received 8 October 2025
Revised 19 October 2025
Accepted 20 October 2025

Abstract

Purpose – The efficient utilization of recycled concrete powder (RCP) has attracted much attention. To break through the limitation of single activation technology of RCP, this study investigates the effects of a mechanical-microwave method on the reactivity of RCP.

Design/methodology/approach – The mechanical properties, hydration products, and pore structure of RCP-incorporated mortar were evaluated.

Findings – The results demonstrate that the combined activation reduces the median particle size of RCP and induces a low-frequency shift in the Si-O-T FT-IR characteristic peaks, signifying depolymerization of the silicate network and formation of highly reactive broken bond sites. Concurrently, decreased Si2p and Al2p binding energies in XPS spectra confirm enhanced surface reactivity. The 28-day strength activity index (SAI) of RCP mortar improved from 65.7 (untreated) to 82.2% under optimal activation conditions (90-min ball milling followed by 10-min microwave irradiation), outperforming solely mechanical activation by 3.6–6.1%. Furthermore, combined activation increased chemically bound water content from 22.8 to 33.7%, accompanied by a low-wavenumber shift in FT-IR peaks of hydration products. The total porosity of RCP mortar decreased from 17.2 to 14.6%, indicating a denser pore structure.

Originality/value – This study explores the feasibility and potential mechanism of mechanical-microwave activation of RCP, aiming to provide valuable insights for the sustainable development of materials. Using activated RCP in cement-based materials reduces the demand for cement and substantially cuts carbon emissions, thereby making a critical contribution to the construction industry's green and low-carbon transition.

Keywords Recycled concrete powder, Mechanical-microwave combing method, Strength activity index, Hydration products, Microstructure

Paper type Research article

1. Introduction

High-efficiency recycling of construction and demolition waste (CDW) represents a pivotal pathway toward sustainable development in civil engineering materials. Recycled concrete powder (RCP), a fine particulate material generated during concrete crushing processes, constitutes 5% – 15% of total CDW by mass. Its indiscriminate landfilling not only consumes valuable land resources but also induces environmental contamination through alkaline

Funding: This research is sponsored by Science and Technology Research and Development Plan of China National Railway Group Co., Ltd. (L2022G009), National Natural Science Foundation of China (52438002), Research Project of China Academy of Railway Science Corporation Limited (2024YJ254) and New Cornerstone Science Foundation through the XPLORER PRIZE.

Railway Sciences
Vol. 4 No. 5, 2025
pp. 625-637
Emerald Publishing Limited
e-ISSN: 2755-0915
p-ISSN: 2755-0907
DOI 10.1108/RS-10-2025-0047

leaching (Xiao, Ma, Sui, Akbarnezhad, & Duan, 2018; Ma *et al.*, 2024; Abriak, Chu, Maherzi, Benzerzour, & Rivard, 2023). RCP predominantly comprises partially hydrated cement particles, calcium silicate hydrate (C-S-H) gels, and reactive silica phases, exhibiting theoretical potential as supplementary cementitious materials (SCMs) (Rocha & Filho, 2024; Ren *et al.*, 2024; Yang *et al.*, 2024a, b). Despite extensive research on RCP activation strategies, critical challenges persist due to its inherent compositional heterogeneity, low reactivity, and high porosity (Kaliyavaradhan, Ling, & Mo, 2020; Ouyang *et al.*, 2025).

The chemical composition of RCP correlates strongly with parent concrete mix designs, typically containing 20–40% CaO, 30–50% SiO_2, and minor Al_2O_3/Fe_2O_3 (Oliveira, Dezen, & Possan, 2020). Its reactivity originates from secondary hydration of residual cement clinker and pozzolanic reactions of siliceous-aluminous phases. However, high proportions of inert components (e.g. quartz, feldspar), irregular particle gradation (Deng *et al.*, 2023), and surface-adsorbed hardened paste significantly impair cementitious system performance: increased water demand and workability loss; retarded early strength development; coarsened pore structure and compromised durability (Duan, Singh, Xiao, & Hou, 2020; Kim & Ubysz, 2024). For instance, Duan *et al.* (2020) reported 116.67% prolonged T_{500} flow time and 40% reduced chloride resistance in self-compacting concrete with 30% RCP substitution, severely restricting practical applications.

Three principal activation approaches have been explored: thermal, mechanical, and chemical treatments. High-temperature calcination (600–800 °C) induces thermal decomposition of inert mineral phases (e.g. $CaCO_3$) in RCP, yielding reactive CaO and amorphous SiO_2 through structural transformations (Wu, Xu, Yang, & Ma, 2021a; Zhang, Zhang, Huang, Yang, & Li, 2022). Chen, Wei, Lei, and Li (2024) achieved 77.4% strength activity index using 700 °C-treated RCP, though energy intensity (>800 kWh/t) and particle agglomeration remain concerns (Ma, Hu, Yao, & Wang, 2023). Mechanical milling reduces particle size (<45 μm) and creates surface defects for enhanced pozzolanicity, yet excessive grinding damages residual cement crystallinity (Meng, Hong, Ying, & Wang, 2021). Alkali activation (e.g. NaOH) and nanomaterial modification (nano-SiO_2) demonstrate effectiveness but increase costs and carbon footprint. Xie, Li, Li, Tang, and Gu (2025) quintupled geopolymer strength via 6% NaOH/750°C treatment, while Wu, Yang, and Ma (2021b) observed 26.4% mortar strength gain at 900 °C despite elevated porosity with >50% RCP. Meng *et al.* (2023) reported 43.4%, 33.3%, and 23.7% 28-day strength improvements using nano-$CaCO_3$, graphene oxide, and nano-SiO_2, respectively, though industrial scalability remains challenging (Liu *et al.*, 2022).

Microwave irradiation emerges as an energy-efficient alternative (80% energy utilization) through dielectric polarization and ionic conduction, achieving rapid heating (>50 °C/min) (Wang, Luo, Yang, & Ding, 2021; Zhang, Tan, Yang, & Luo, 2024). Polar molecules (Ca$(OH)_2$, C-S-H) preferentially absorb microwaves, inducing lattice vibration and phase transformation. Zhang, Qiao, and Yu (2015) documented 30% reactivity enhancement via 800 W microwave-induced quartz amorphization. Microwave-induced microcracks facilitate subsequent grinding for submicron powders (Guan, Chen, Zhu, & Gao, 2021), while Yang *et al.* (2024c) observed 18% ITZ porosity reduction and 25% C-S-H increase after 490 W/10 min treatment. Mechanical-microwave synergy overcomes single-mode limitations: pre-milling increases surface area for microwave interaction, while microwave-induced bond cleavage releases reactive phases. Xu, Kang, Wu, Gong, and Xiao (2021) achieved 108.18% geopolymer strength improvement via 10 min milling + 750 °C microwave, outperforming individual treatments. Feng *et al.* (2023) enhanced CO_2 sequestration by 50% through mechano-carbonation without alkali additives.

This paper systematically investigates the effects of mechanical-microwave combing method on the phase composition, hydration activity, and microstructural evolution of RCP. It elucidates the multi-scale mechanisms of mechanical-microwave synergism during the activation process of RCP and establishes a synergistic system of “mechanical refinement-chemical activation-performance enhancement,” thereby promoting the development of recycling technologies for CDW.

2. Experiment

2.1 Materials

The raw materials comprised RCP derived from C40-grade concrete, ordinary Portland cement (P.O 42.5), tap water, and reference sand. The particle size distributions of cement and RCP, as determined by laser diffraction analysis, are presented in Figure 1, while the chemical compositions obtained via XRF spectrometry are summarized in Table 1.

2.2 Mechanical-microwave activation method

Mechanical ball milling of RCP effectively refined its particle size distribution and increased its specific surface area. As indicated in Table 1, the RCP contains abundant polar oxides such as SiO_2 and Al_2O_3. Under microwave electromagnetic fields and thermal effects, these components facilitated the cleavage of siloxane (Si-O) and aluminate (Al-O) bonds, thereby enhancing the reactivity. This study systematically investigated the effects of ball milling time (30, 60, and 90 min) and microwave irradiation time (5, 10, and 15 min) on RCP activation. A SYM-500 cement ball mill (Hebei Kexi Instrument Equipment Co., Ltd., China; motor power: 1.5 kW, rotational speed: 48 rpm) was employed for mechanical activation. Subsequent microwave treatment was conducted using a Galanz WP700P21 microwave oven at 700 W power. The detailed activation protocols are summarized in Table 2.

2.3 Preparation of recycled mortar

RCP-incorporated mortar specimens (40 mm × 40 mm × 160 mm) were prepared according to GB/T 17671-2021 with a water-to-cement ratio of 0.5, where RCP replaced 30% of cement by

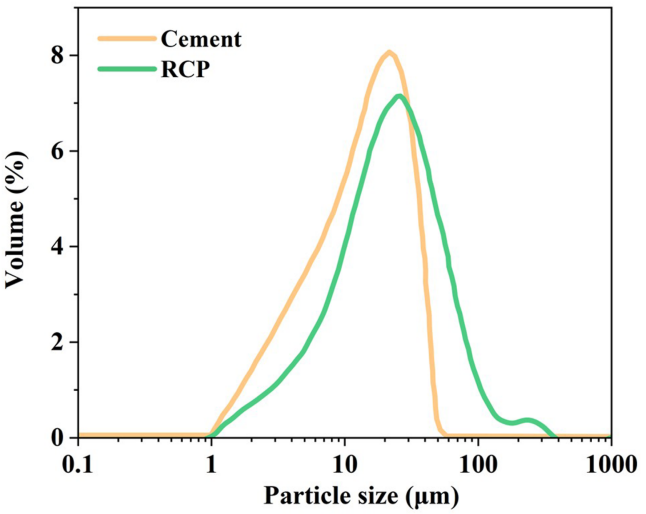

Figure 1. The particle size distribution of cement and recycled concrete powder. **Source(s):** Authors' own work

Table 1. Chemical composition of cement and RCP (%)

Type	CaO	SiO_2	Al_2O_3	Fe_2O_3	MgO	SO_3
Cement	57.68	21.62	6.11	3.23	3.32	2.39
RCP	36.69	33.43	9.70	9.55	4.51	0.58

Source(s): Authors' own work

Table 2. Mechanical-microwave activation test system for RCP

Type	Ball milling time (min)	Microwave time (min)
RCP1	0	0
RCP2	30	0
RCP3	30	15
RCP4	60	0
RCP5	60	15
RCP6	90	0
RCP7	90	5
RCP8	90	10
RCP9	90	15

Source(s): Authors' own work

mass. After demolding at 24 h, specimens were cured in a standard chamber. Three specimens per mixture were tested at 3, 7, and 28 days. The mortar mix proportions are detailed in Table 3.

2.4 Test method

2.4.1 Mortar strength. The flexural and compressive strengths of RCP-incorporated mortar specimens were measured at 3, 7, and 28 days of curing using three replicates per group, following GB/T 17671-2021. The strength activity index (SAI) of RCP was calculated according to GB/T 1596-2017 using Eq. (1):

$$H = \frac{R}{R_0} \times 100\% \tag{1}$$

where H denotes the SAI, R represents the 28-day compressive strength of RCP-blended mortar (MPa), and R_0 is the 28-day compressive strength of the reference mortar (MPa).

2.4.2 Median particle size. The median particle size of RCP was determined using a Mastersizer 2000 laser granulometer (Malvern Panalytical), with triplicate measurements averaged for each sample.

2.4.3 Specific surface area. The specific surface area was tested per GB/T 8074-2008.

2.4.4 XRF. Chemical compositions of cement and RCP were analyzed via XRF spectroscopy using an ARL PERFORM'X spectrometer (Thermo Fisher Scientific).

2.4.5 FT-IR. FT-IR spectroscopy was conducted on a Bruker Vertex 70 spectrometer (Horiba) with a scanning range of 400–2000 cm^{-1} and 4 cm^{-1} resolution.

2.4.6 XPS. Surface chemical states were analyzed via XPS (ESCALAB 250Xi, ThermoFisher Scientific), focusing on Si_{2p}, Al_{2p}, and $C1_s$ orbitals.

Table 3. Mix proportions of recycled mortar

Type	Cement (g)	RCP (g)	Reference sand (g)	Water (g)	W/C	Type of RCP
MRP-0	450	0	1,350	225	0.5	–
MRP-1	315	135				RCP1
MRP-2	315	135				RCP2
MRP-3	315	135				RCP3
MRP-4	315	135				RCP4
MRP-5	315	135				RCP5
MRP-6	315	135				RCP6
MRP-7	315	135				RCP7
MRP-8	315	135				RCP8
MRP-9	315	135				RCP9

Source(s): Authors' own work

2.4.7 TG-DTG. The degree of hydration of the recycled mortar was tested using a Q5000IR thermogravimetric analyzer manufactured by TA INSTRUMENTS. The scanning range was from room temperature to 900 °C, with a heating rate of 10 °C/min.

2.4.8 MIP. The pore structure of the recycled mortar was tested using a MicroActive AutoPore V 9600 mercury injection porosimeter manufactured by Micromeritics.

3. Result and discussion

3.1 Performance of RCP

3.1.1 Median particle size and specific surface area. Figure 2 presents the median particle size (d_{50}) and specific surface area of cement and RCP under different activation regimes. Mechanical activation effectively optimized particle size distribution, while microwave irradiation demonstrated supplementary refinement capability. The untreated RCP exhibited a d_{50} of 21.833 μm, representing a 54.1% increase compared to cement (Figure 2(a)). Ball milling for 30, 60, and 90 min reduced d_{50} values to 17.226 μm, 17.026 μm, and 16.582 μm, respectively. Extended microwave exposure further decreased d_{50} through differential dielectric responses of mineral constituents, generating stress gradients and microcracks under thermal-electrical coupling effects.

As shown in Figure 2(b), ball milling for 30 min induced a 132.3% specific surface area enhancement. However, prolonged grinding beyond 60 min stabilized specific surface area values, indicating dynamic equilibrium between particle fragmentation and agglomeration. This suggests approaching the comminution limit under current mechanical parameters.

3.1.2 FT-IR analysis. Figure 3 shows FTIR spectra of activated recycled powders. In the infrared spectrum, the peak around 1,448 cm^{-1} represents the bending vibration of C-O-C.

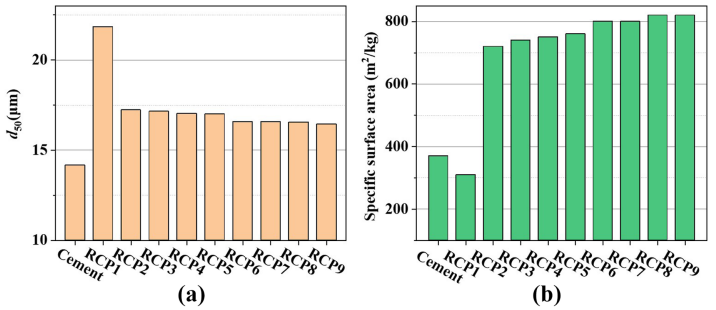

Figure 2. Median particle size and specific surface area of RCP. **Note(s):** (a) median particle size; (b) specific surface area. **Source(s):** Authors' own work

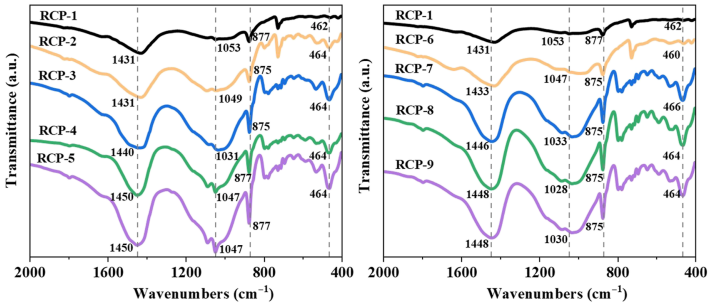

Figure 3. FT-IR of RCP. **Source(s):** Authors' own work

The infrared absorption peaks within the range of 850 cm^{-1} to 1,200 cm^{-1} primarily correspond to the stretching vibration peaks of Si-O-T (where T = Si, Al). The peak at approximately 464 cm^{-1} represents the in-plane bending vibration peak of Si-O-Si. The untreated sample exhibited maximum absorption at 1,053 cm^{-1}. Ball-milled samples showed progressive peak shifts to 1,049 cm^{-1} (30 min), 1,047 cm^{-1} (60 min), and 1,047 cm^{-1} (90 min). Microwave irradiation induced more pronounced low-frequency shifts to 1,030 cm^{-1}, attributable to lattice distortion from Al^{3+}/Ca^{2+} substitution in SiO_4 tetrahedra. Microwave-induced dipole realignment weakened chemical bonds through non-contact energy transfer, facilitating depolymerization of silicate networks.

3.1.3 XPS analysis. Based on the principle of XPS, the electron binding energy of surface element is related to the chemical environment of the atomic species at the surface. Furthermore, since the hydraulic activity of cementitious materials predominantly occurs at the particle surface, there exists a certain correlation between the surface electron binding energy of materials and the cementitious reactivity. Li, Sun, Tie, and Xiao (2006) proposed the use of Si_{2p} and Al_{2p} surface electron binding energies to evaluate the cementitious reactivity of coal gangue-based silico-alumina materials, suggesting that lower Si_{2p} and Al_{2p} binding energies indicate higher reactivity of the coal gangue. Luo, Yuan, and Zhu (1985) pointed out that materials with smaller Si_{2p} binding energies exhibit stronger reactivity, while those with higher total silicon and aluminum content at the surface show weaker reactivity, and materials with higher calcium content at the surface exhibit stronger reactivity. Following mechanical-microwave treatment, XPS was employed to measure the Si_{2p} and Al_{2p} binding energies of RCP.

Figure 4 depicts the Si_{2p} binding energies of the RCP. The untreated RCP exhibited the highest Si_{2p} binding energy of 102.90 eV. As ball milling time increased, the Si_{2p} binding energy of the RCP without microwave irradiation initially decreased and then remained relatively constant, with RCP-2, RCP-4, and RCP-6 exhibiting Si_{2p} binding energies of 102.72 eV, 102.58 eV, and 102.60 eV, respectively. However, after 15 minutes of microwave irradiation, the Si_{2p} binding energy further decreased. RCP-3, RCP-5, and RCP-9 had Si_{2p} binding energies of 102.53 eV, 102.50 eV, and 102.46 eV, respectively, representing reductions of 0.19 eV, 0.08 eV, and 0.14 eV compared to mechanical activation alone. After 90 minutes of ball milling, as microwave irradiation time increased, the Si_{2p} binding energy of the RCP also showed a trend of initial decrease followed by stability, with RCP-7, RCP-8, and RCP-9 exhibiting Si_{2p} binding energies that were 0.08 eV, 0.15 eV, and 0.14 eV lower than RCP-6, respectively.

Figure 5 presents the Al_{2p} binding energies of the RCP before and after activation. RCP-1 had the highest Al_{2p} surface electron binding energy of 74.65 eV. As ball milling time increased, the Al_{2p} binding energy of the RCP without microwave irradiation gradually decreased, with RCP-2, RCP-4, and RCP-6 exhibiting Al_{2p} binding energies of 74.47 eV, 74.45 eV, and 74.37 eV, respectively. After 15 minutes of microwave irradiation, the Al_{2p} binding energies decreased by 0.18 eV, 0.22 eV, and 0.15 eV compared to ball milling alone. After 90 minutes of ball milling, as microwave irradiation time increased, the Al_{2p} binding

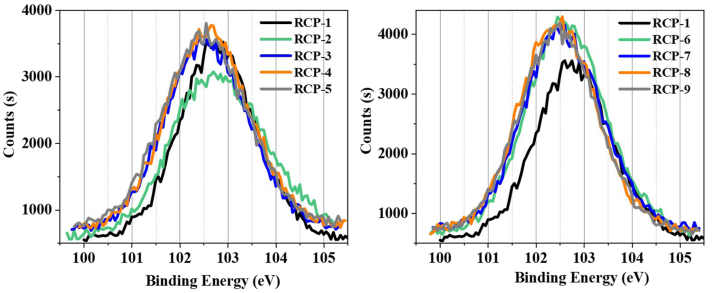

Figure 4. Si_{2p} binding energy of RCP. **Source(s):** Authors' own work

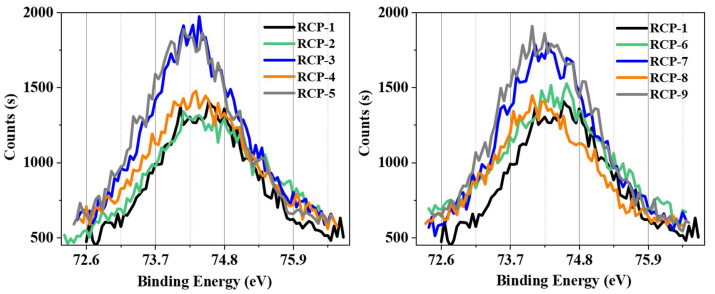

Figure 5. Al_{2p} binding energy of RCP. **Source(s):** Authors' own work

energy of the RCP also exhibited a trend of initial decrease followed by stability, with RCP-7, RCP-8, and RCP-9 exhibiting Al_{2p} binding energies that were 0.08 eV, 0.22 eV, and 0.15 eV lower than RCP-6, respectively. The binding energy of aluminum is related to its coordination (Black *et al.*, 2003), with tetrahedrally coordinated aluminum typically having a binding energy range of 73.4 eV to 74.55 eV, and hexahedrally coordinated aluminum having a binding energy range of 74.1 eV to 75.0 eV. After microwave irradiation, hexacoordinated aluminum in the RCP gradually transformed into tetracoordinated aluminum, resulting in decreased binding energy and enhanced reactivity.

3.2 Performance of recycled mortar

3.2.1 Mechanical property. Figures 6 and 7 are the flexural and compressive strengths of recycled mortar at 3, 7, and 28 days, respectively, while Figure 8 presents the SAI of recycled

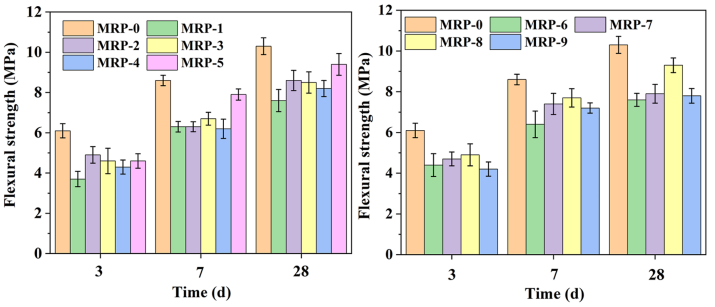

Figure 6. Flexural strength of recycled mortar. **Source(s):** Authors' own work

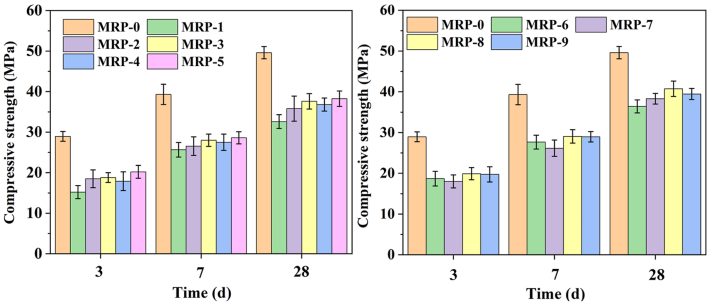

Figure 7. Compressive strength of recycled mortar. **Source(s):** Authors' own work

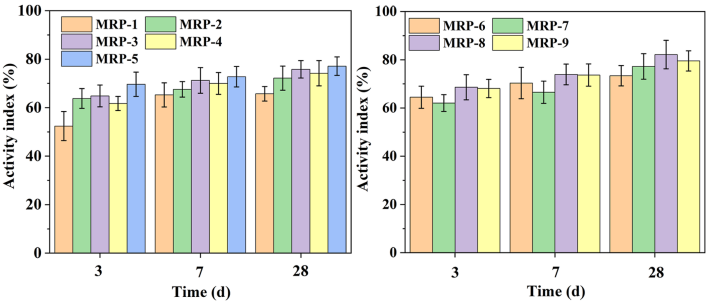

Figure 8. Strength activity index of recycled mortar. **Source(s):** Authors' own work

mortar. At 28 days, the reference mortar (MRP-0) achieved compressive and flexural strengths of 49.6 MPa and 10.3 MPa, respectively. In contrast, the untreated recycled powder mortar (MRP-1) exhibited significantly lower values of 32.6 MPa (compressive strength) and 7.6 MPa (flexural strength). For non-microwave-treated mortars, strength initially increased but subsequently declined with prolonged ball milling. The SAIs for MRP-2, MRP-4, and MRP-6 were 72.2%, 74.2%, and 73.4%, respectively. Conversely, microwave irradiation (15 min) coupled with ball milling progressively enhanced strength, yielding SAIs of 75.8% (MRP-3), 77.1% (MRP-5), and 79.5% (MRP-9). The combined mechanical-microwave activation outperformed mechanical treatment alone, improving SAIs by 3.6%, 2.9%, and 6.1% at 30, 60, and 90 min of ball milling, respectively. Further optimization revealed that extending microwave exposure beyond 15 min after 90 min ball milling caused SAI reduction.

The strength evolution correlates directly with microstructural modifications induced by activation. During mechanical-microwave treatment, polar oxides (e.g. SiO_2, Al_2O_3) in RCP absorb microwave energy, facilitating cleavage of Si-O and Al-O bonds. This releases reactive Si^{4+} and Al^{3+} ions, which interact with evaporable water to form hydration products (CH, C-(A)-S-H, gypsum, and ettringite), thereby accelerating cement hydration. These phenomena align with observed reductions in SiO_2/Al_2O_3 content and low-frequency shifts of Si-O-T (T = Si/Al) stretching vibrations.

However, excessive microwave exposure (15 min) after 90 min ball milling increased the median particle size due to prolonged thermal effects. Elevated temperatures degraded hydration products (C-(A)-S-H, gypsum, and ettringite), diminishing powder reactivity and ultimately compromising strength. This underscores the necessity for precise control over microwave duration to balance activation efficacy and thermal degradation.

3.2.2 TG-DTG analysis. Figure 9 presents the TG-DTG curves of recycled mortar. The TG curves enable quantitative determination of C-S-H, $Ca(OH)_2$, $CaCO_3$ contents and chemically bound water. In the TG curve of recycled mortar, a distinct mass loss peak appears between

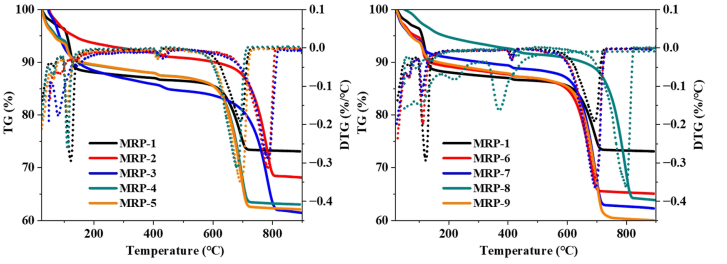

Figure 9. TG-DTG of recycled mortar. **Source(s):** Authors' own work

30–200 °C, corresponding to dehydration of gypsum and calcium silicate hydrate (C-S-H). The second mass loss stage observed between 350–500 °C can be attributed to dehydroxylation of calcium hydroxide. The third decomposition stage in the range of 500–720 °C represents decarbonation of calcium carbonate. The chemically bound water content, calculated from mass loss between 105–900 °C, serves as an indicator of hydration degree (Gómez-Zamorano & Escalante-García, 2010).

Figure 10 illustrates the chemically bound water contents of recycled mortar. The MRP-1 group exhibited a relatively low bound water content of 22.8%. With extended ball milling duration, the chemically bound water content in non-microwave-treated recycled mortar initially increased then decreased, reaching 27.8%, 30.9%, and 29.2% for MRP-2, MRP-4, and MRP-6 respectively. Notably, the combined mechanical-microwave activation enhanced the bound water content by 3.1%, 0.4%, and 4.3% compared to sole mechanical activation at 30-min, 60-min, and 90-min milling durations. Prolonged microwave exposure after 90 min ball milling progressively increased and stabilized the bound water content, with values of 29.2%, 31.6%, 33.7%, and 33.5% recorded for MRP-6 through MRP-9. These experimental findings demonstrate that under the proposed activation regime, recycled powder effectively accelerates cement hydration kinetics and promotes hydration product formation. This microstructural enhancement mechanism contributes to improved matrix densification and consequent mechanical performance enhancement in recycled mortar systems.

3.2.3 FT-IR analysis. Figure 11 displays the FTIR spectra of recycled mortar. The characteristic absorption bands of cement hydration products predominantly appear in the 850–1,200 cm^{-1} region, corresponding to stretching vibrations of Si-O-T bonds (T = Si or Al). The peak at 1,431 cm^{-1} signifies bending vibrations of carbonate ions (CO_3^{2-}), confirming calcium carbonate presence in the samples. This carbonation phenomenon likely originates from prolonged environmental exposure of the parent concrete materials during

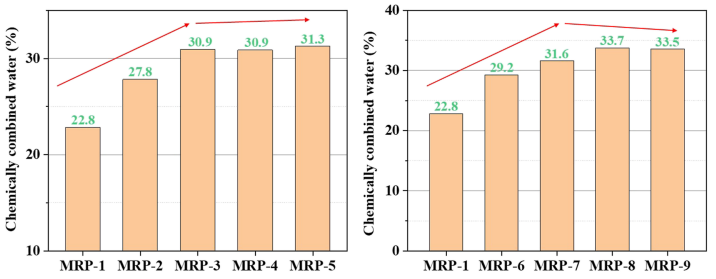

Figure 10. Chemically combined water content of recycled mortar. **Source(s):** Authors' own work

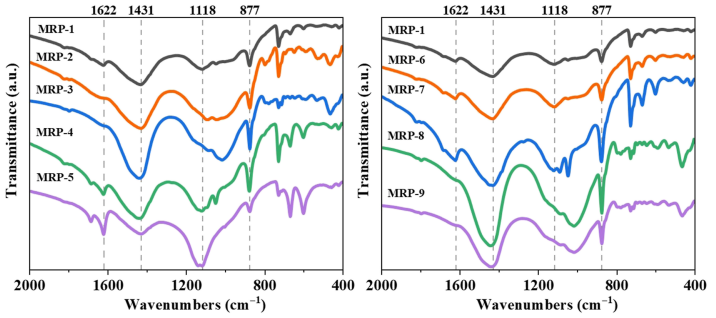

Figure 11. FT-IR of recycled mortar. **Source(s):** Authors' own work

service life. The absorption band at 1,622 cm^{-1} is associated with H-O-H bending vibrations of water molecules.

Within the critical hydration reaction zone (850–1,200 cm^{-1}), the spectral features correspond to C-S-H gel formation. The control group (unactivated MRP) exhibited characteristic peaks at 877 cm^{-1} and 1,118 cm^{-1}. Activation treatment induced distinct peak shifts toward lower wave numbers, which may be attributed to isomorphous substitution of Si by Al or Ca in the Si-O-T network. This structural modification suggests increased Al incorporation within C-(A)-S-H gels, consistent with enhanced Al^{3+} dissolution from microwave-activated MRP. The observed spectral alterations demonstrate that combined mechanical-microwave activation effectively modifies the atomic-scale structure of hydration products through aluminum phase mobilization.

3.2.4 MIP analysis. Figure 12 illustrates the pore size distribution of recycled mortar, categorized based on their impacts on concrete performance: innocuous pores (0–20 nm), less harmful pores (20–100 nm), harmful pores (100–200 nm), and multi-harmful pores (>200 nm) (Chen, Zou, Zhou, Hu, & Mao, 2025; Li *et al.*, 2025). The untreated control group (MRP-1) exhibited the highest total porosity of 17.2%. With extended ball milling duration, non-microwave-treated recycled mortar maintained relatively stable porosity levels (17.0%, 16.9%, and 16.9% for MRP-2, MRP-4, and MRP-6 respectively), while demonstrating progressive increases in beneficial pore fractions - the combined volume of innocuous and less harmful pores rose from 11.6% to 12.9%. This pore refinement can be attributed to particle size reduction and increased specific surface area through mechanical activation, enhancing the filler effect for matrix densification.

Microwave-assisted activation induced more pronounced porosity reduction. Specimens subjected to 15-min microwave radiation (MRP-3, MRP-5, MRP-9) showed decreasing porosity with milling duration (16.8%, 16.2%, and 16.0% respectively), accompanied by beneficial pore fractions of 11.3–12.1%. Comparative analysis revealed the superior efficacy of combined mechanical-microwave activation, achieving porosity reductions of 0.2%, 0.7%, and 0.9% over sole mechanical treatment at 30-min, 60-min, and 90-min milling intervals. Post 90-min milling, porosity evolution exhibited a characteristic "V-shaped" trend with prolonged microwave exposure.

This performance enhancement stems from synergistic activation mechanisms: 1) Microwave-thermal coupling significantly improves pozzolanic reactivity through intensified CH liberation, facilitating Si-O and Al-O bond cleavage that promotes network depolymerization and ionic dissolution (Ca^{2+}, Al^{3+}, SiO_4^{4-}); 2) Secondary hydration reactions generate additional C-(A)-S-H gels and ettringite, effectively filling >200 nm pores through a dual pore-refinement mechanism - physical packing by ultrafine particles and chemical pore infilling by hydration products. The resultant microstructural optimization directly correlates with the observed mechanical strength enhancement in activated recycled mortar systems.

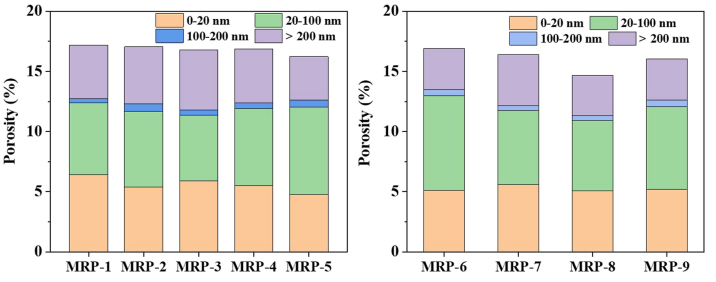

Figure 12. Pore size distribution of recycled mortar. **Source(s):** Authors' own work

4. Conclusion

This study investigates the effects of mechanical ball milling and microwave irradiation on the reactivity of RCP, elucidating the activation mechanism of the mechano-microwave approach. The principal conclusions are summarized as follows:

(1) The micro-mechanism of mechanical-microwave activated RCP is revealed. A low-frequency shift in the Si-O-T bond IR peak signifies weakened bond strength, facilitating depolymerization of the siloxane network and generating highly reactive sites. Prolonged activation leads to an initial decrease and subsequent stabilization of Si_{2p} and Al_{2p} binding energies, while the conversion of Al(VI) to Al(IV) further enhances chemical reactivity.

(2) The mechanical-microwave activation method enhances the mechanical properties of recycled mortar. This combined technique is superior to mechanical activation alone, as evidenced by the increases in the strength activity index by 3.6%, 2.9%, and 6.1% after 30, 60, and 90 minutes of ball milling, respectively. The optimal activation efficiency is achieved with a combination of 90-min ball milling and 10-min microwave irradiation.

(3) The hybrid activation method enhances hydration products in recycled mortar. Chemically bound water content progressively increases and stabilizes with activation duration, showing 0.4% - 4.3% improvement over mechanical activation alone. FT-IR analysis reveals peak shifts toward lower wave numbers in the primary hydration reaction region (850–1,200 cm^{-1}). Porosity decreases with activation time, yielding a denser pore structure.

(4) The activation of RCP and its conversion into a cementitious material serve as a critical step in advancing construction waste management from “partial recycling” to “full-component recycling”. The application of activated RCP in cement-based composites effectively replaces cement, leading to a substantial reduction in carbon emissions. This approach represents a pivotal pathway towards achieving a green and low-carbon transformation in the construction industry.

This study presents a preliminary investigation into the mechanical-microwave activation of RCP. Due to the use of ball milling and microwave equipment with limited power, it is recommended that high-power industrial apparatus be employed for activation in future industrial-scale applications.

References

Abriak, Y., Chu, D. C., Maherzi, W., Benzerzour, M., & Rivard, P. (2023). Influence of fine recycled concrete aggregates use on the hydration kinetics and mechanical–microstructural properties of hydrated cement: Experimental and numerical approaches. *Construction and Building Materials*, *408*, 133769. doi: 10.1016/j.conbuildmat.2023.133769.

Black, L., Stumm, A., Garbev, K., Stemmermann, P., Hallam, K. R., & Allen, G. C. (2003). X-ray photoelectron spectroscopy of the cement clinker phases tricalcium silicate and β-dicalcium silicate. *Cement and Concrete Research*, *33*(10), 1561–1565. doi: 10.1016/S0008-8846(03)00097-8.

Chen, L., Wei, M., Lei, N., & Li, H. (2024). Effect of chemical–thermal activation on the properties of recycled fine powder cementitious materials. *Case Studies in Construction Materials*, *20*, e02956. doi: 10.1016/j.cscm.2024.e02956.

Chen, F., Zou, C. Y., Zhou, Y. M., Hu, S. T., & Mao, J. H. (2025). Correlation analysis of abrasion resistance of rubber concrete with microstructure and pore structure. *Construction and Building Materials*, *475*, 141211. doi: 10.1016/j.conbuildmat.2025.141211.

Deng, X., Li, J., Lu, Z. Y., Zhang, J. J., Luo, K., Niu, Y. H., . . . He, K. W. (2023). Rheological and early hydration of cementitious material containing recycled concrete powders collected from recycled aggregates. *Construction and Building Materials*, *393*, 132108. doi: 10.1016/j.conbuildmat.2023.132108.

Duan, Z. H., Singh, A., Xiao, J. Z., & Hou, S. D. (2020). Combined use of recycled powder and recycled coarse aggregate derived from construction and demolition waste in self-compacting concrete. *Construction and Building Materials*, *254*, 119323. doi: 10.1016/j.conbuildmat.2020.119323.

Feng, Y., Li, J., Zhang, B., Fu, H., Chen, W., Xue, Z., . . . Xie, J. H. (2023). Concrete improvement incorporating recycled powder and aggregates treated via a combination of calcination and carbonation: The impact behaviors. *Journal of Cleaner Production*, *418*, 138069. doi: 10.1016/j.jclepro.2023.138069.

Gómez-Zamorano, L. Y., & Escalante-García, J. I. (2010). Effect of curing temperature on the nonevaporable water in Portland cement blended with geothermal silica waste. *Cement and Concrete Composites*, *32*(8), 603–610. doi: 10.1016/j.cemconcomp.2010.07.004.

Guan, X., Chen, J. X., Zhu, M. Y., & Gao, J. (2021). Performance of microwave-activated coal gangue powder as auxiliary cementitious material. *Journal of Materials Research and Technology*, *14*, 2799–2811. doi: 10.1016/j.jmrt.2021.08.106.

Kaliyavaradhan, S. K., Ling, T. L., & Mo, K. H. (2020). Valorization of waste powders from cement-concrete life cycle: A pathway to circular future. *Journal of Cleaner Production*, *268*, 122358. doi: 10.1016/j.jclepro.2020.122358.

Kim, J., & Ubysz, A. (2024). Thermal activation of multi-recycled concrete powder as supplementary cementitious material for repeated and waste-free recycling. *Journal of Building Engineering*, *98*, 111169. doi: 10.1016/j.jobe.2024.111169.

Li, H. J., Sun, H. H., Tie, X. C., & Xiao, X. J. (2006). Study on activity evaluation of thermal treated gangue. *Journal of China Coal Society*, *31*(5), 654–658. doi: CNKI:SUN:MTXB.0.2006-05-023.

Li, B. X., Yang, H. T., Chen, X., Ni, M. X., Ye, W. D., & Zhang, Y. L. (2025). Enhancement of concrete properties through roller grinding technique for recycled sand. *Construction and Building Materials*, *492*, 142992. doi: 10.1016/j.conbuildmat.2025.142992Getrightsandcontent.

Liu, X. Y., Liu, L., Lyu, K., Li, T. Y., Zhao, P. Z., Liu, R. D., . . . Shah, S. P. (2022). Enhanced early hydration and mechanical properties of cement-based materials with recycled concrete powder modified by nano-silica. *Journal of Building Engineering*, *50*, 104175. doi: 10.1016/j.jobe.2022.104175.

Luo, X. H., Yuan, R. Z., & Zhu, X. A. (1985). Study of the surface reactivity of cemental materials particles by XPS. *Chinese Journal of Vacuum Science and Technology*, *5*(1), 30–32. doi: 10.13922/j.cnki.cjovst.1985.01.006.

Ma, Z., Hu, R., Yao, P., & Wang, C. (2023). Utilizing heat-mechanical synergistic treatment for separating concrete waste into high-quality recycled aggregate, active recycled powder and new concrete. *Journal of Building Engineering*, *68*, 106161. doi: 10.1016/j.jobe.2023.106161.

Ma, Z. H., Jiang, Y., He, J. H., Shen, P. L., Qin, Q. L., Gu, Z. J., . . . Poon, C. S. (2024). Revealing the connection between carbonation regimes and early pozzolanic reactivity of recycled concrete powder: Impact of composition and microstructure. *Cement and Concrete Research*, *186*, 107697. doi: 10.1016/j.cemconres.2024.107697.

Meng, T., Hong, Y., Ying, K., & Wang, Z. (2021). Comparison of technical properties of cement pastes with different activated recycled powder from construction and demolition waste. *Cement and Concrete Composites*, *120*, 104065. doi: 10.1016/j.cemconcomp.2021.104065.

Meng, T., Dai, D., Jia, Y., Ying, K., Meng, R., & Hong, Y. (2023). Comparative study of nanomaterials activated recycled powders from demolition and decoration wastes as supplementary cementitious material. *Case Studies in Construction Materials*, *19*, e02543. doi: 10.1016/j.cscm.2023.e02543.

Oliveira, T. C. F., Dezen, B. G. S., & Possan, E. (2020). Use of concrete fine fraction waste as a replacement of Portland cement. *Journal of Cleaner Production*, *273*, 123126. doi: 10.1016/j.jclepro.2020.123126.

Ouyang, X. W., Li, X. F., Li, J. M., Ma, Y. W., Zhang, M. Z., Li, Z. J., & Fu, J. Y. (2025). Multiscale microstructure and reactivity evolution of recycled concrete fines under gas-solid carbonation. *Cement and Concrete Composites*, *157*, 105903. doi: 10.1016/j.cemconcomp.2024.105903.

Ren, X., Yang, J. P., Chen, W. L., Huang, Y. F., Wang, G., Niu, J. W., & Wu, J. L. (2024). Effect of recycled concrete powder-cement composite coating modification on the properties of recycled concrete aggregate and its concrete. *Construction and Building Materials*, *444*, 137860. doi: 10.1016/j.conbuildmat.2024.137860.

Rocha, J. H. A., & Filho, R. D. T. (2024). Microstructure, hydration process, and compressive strength assessment of ternary mixtures containing Portland cement, recycled concrete powder, and metakaolin. *Journal of Cleaner Production*, *434*, 140085. doi: 10.1016/j.jclepro.2023.140085.

Wang, Y. L., Luo, S. Q., Yang, L., & Ding, Y. H. (2021). Microwave curing cement-fly ash blended paste. *Construction and Building Materials*, *282*, 122685. doi: 10.1016/j.conbuildmat.2021.122685.

Wu, H. X., Xu, J. G., Yang, D. Y., & Ma, Z. M. (2021a). Utilizing thermal activation treatment to improve the properties of waste cementitious powder and its newmade cementitious materials. *Journal of Cleaner Production*, *322*, 129074. doi: 10.1016/j.jclepro.2021.129074.

Wu, H. X., Yang, D. Y., & Ma, Z. M. (2021b). Micro-structure, mechanical and transport properties of cementitious materials with high-volume waste concrete powder and thermal modification. *Construction and Building Materials*, *313*, 125477. doi: 10.1016/j.conbuildmat.2021.125477.

Xiao, J. Z., Ma, Z. M., Sui, T. B., Akbarnezhad, A., & Duan, Z. H. (2018). Mechanical properties of concrete mixed with recycled powder produced from construction and demolition waste. *Journal of Cleaner Production*, *188*, 720–731. doi: 10.1016/j.jclepro.2018.03.277.

Xie, J., Li, C., Li, B., Tang, J., & Gu, F. (2025). Thermal-alkaline activation enhances the mechanical properties of low-activity recycled concrete powder-derived geopolymers. *Construction and Building Materials*, *463*, 140020. doi: 10.1016/j.conbuildmat.2025.140020.

Xu, J., Kang, A. H., Wu, Z. G., Gong, Y. F., & Xiao, P. (2021). The effect of mechanical-thermal synergistic activation on the mechanical properties and microstructure of recycled powder geopolymer. *Journal of Cleaner Production*, *327*, 129477. doi: 10.1016/j.jclepro.2021.129477.

Yang, Y. G., Xu, J. K., Gao, P., Zhan, B. G., Yu, Q. J., Ni, M. X., & Zhang, Y. S. (2024a). Study on the hydration characteristics and mechanical properties of recycled powder-slag powder-cement system. *Case Studies in Construction Materials*, *21*, e03952. doi: 10.1016/j.cscm.2024.e03952.

Yang, Y. G., Xu, J. K., Zhan, B. G., Gao, P., Yu, Q. J., Li, R., . . . Zhang, Y. S. (2024b). Study on hydration characteristics and mechanism of recycled powder-cement binary and multivariate systems. *Construction and Building Materials*, *420*, 135646. doi: 10.1016/j.conbuildmat.2024.135646.

Yang, Y. G., Tian, D. Y., Gao, P., Zhan, B. G., Yu, Q. J., Wang, P. F., . . . Ding, Z. W. (2024c). Study on the effect and mechanism of microwave excitation on the activity of recycled powder of waste concrete. *Construction and Building Materials*, *429*, 136410. doi: 10.1016/j.conbuildmat.2024.136410.

Zhang, Z. Y., Qiao, X. C., & Yu, J. G. (2015). Aluminum release from microwave-assisted reaction of coal fly ash with calcium carbonate. *Fuel Processing Technology*, *134*, 303–309. doi: 10.1016/j.fuproc.2014.12.050.

Zhang, D., Zhang, S., Huang, B., Yang, Q., & Li, J. (2022). Comparison of mechanical, chemical, and thermal activation methods on the utilisation of recycled concrete powder from construction and demolition waste. *Journal of Building Engineering*, *61*, 105295. doi: 10.1016/j.jobe.2022.105295.

Zhang, S. X., Tan, H. B., Yang, L., & Luo, S. Q. (2024). Impact of microwave radiation on recycled concrete powder in cement-based materials: Structure, hydration activity and mechanism. *Journal of Building Engineering*, *86*, 108864. doi: 10.1016/j.jobe.2024.108864.

Corresponding author
Henan Shi can be contacted at: hnshicars@163.com

Henan Shi received his M.S. degree from the School of Civil Engineering and Architecture at Beijing Jiaotong University, and is currently a Ph. D. candidate in Bridge and Tunnel Engineering at the China Academy of Railway Sciences. His research focuses on the application of recycled concrete in railway engineering, and he has authored 10 SCI/EI-indexed papers.